Conformational Study of a Potent Human Renin Inhibitor: X-Ray Crystal Structure of Isopropyl (2*R*,3*S*)-4-Cyclohexyl-2-hydroxy-3-{*N*-[(2*R*)-2-morpholinocarbonylmethyl-3-(1-naphthyl)propionyl]-L-histidylamino}butyrate (KRI-1314), a Pentapeptide Analogue with Amino Acid Sequence Corresponding to the Cleavage Site of Angiotensinogen

Mitsunobu Doi,[a] Yasuko In,[a] Masatoshi Inoue,[a] Toshimasa Ishida,*[,a] Kinji Iizuka,[b] Kenji Akahane,[b] Hiromu Harada,[b] Hideaki Umeyama[c] and Yoshiaki Kiso*[,d]

[a] *Department of Physical Chemistry, Osaka University of Pharmaceutical Sciences, 2-10-65 Kawai, Matsubara, Osaka 580, Japan*

[b] *Central Research Laboratories, Kissei Pharmaceutical Co., Ltd., Yoshino, Matsumoto, Nagano 339, Japan*

[c] *School of Pharmaceutical Sciences, Kitasato University, Shirokane, Minato-ku, Tokyo 108, Japan*

[d] *Department of Medicinal Chemistry, Kyoto Pharmaceutical University, Yamashita-ku, Kyoto 607, Japan*

A potent inhibitor of renin, isopropyl (2*R*,3*S*)-4-cyclohexyl-2-hydroxy-3-{*N*-[(2*R*)-2- morpholinocarbonylmethyl-3-(1-naphthyl)propionyl]-L-histidylamino}butyrate (KRI-1314), was crystallized as a cinnamic acid salt. The crystal structure of KRI-1314 was determined by X-ray analysis, and the conformation is discussed in relation to the inhibitory activity. The backbone chain of the molecule was largely twisted at the unusual amino acid residue of cyclohexylnorstatine. The observed conformation was compared with that of the model pentapeptide corresponding to the scissile site of angiotensinogen. The stacking interaction was formed between the histidine side-chains related by the crystallographic 2-fold screw axis. The histidine imidazole rings were further fixed by hydrogen bonds with the cinnamic acid. The water molecule of crystallization mediated the hydrogen-bonding bridge of the cinnamic acid with the hydroxy oxygen of the cyclohexylnorstatine. Such interactions appear to be very important in considerations of inhibitor- or substrate-binding mechanisms against renin.

Renin is an aspartic protease (EC 3.4.23.15), which generates a decapeptide of angiotensin I (Asp-Arg-Val-Try-Ile-His-Pro-Phe-His-Leu) from the circulation glycoprotein, angiotensinogen. Angiotensin I is further cleaved by angiotensin-converting enzymes (ACE) to yield the dipeptide His-Leu and angiotensin II (octapeptide).[1] Angiotensin II exhibits strong vasoconstrictor activity and correlates with the maintenance of normal blood pressure.[2] Therefore, the route of the renin–angiotensin system has been a target for antihypertensive therapy.[3]

It is well known that captopril[4] and enalapril[5] are potent ACE inhibitors. The hypertensive state which is related to the imbalance of the renin–angiotensin pathway is improved by the administration of these and relating drugs. Many investigations have been focussed on peptide inhibitors effective against renin. Most of them possess a partial amino acid sequence corresponding to the scissile P5-P3′ site* of angiotensinogen.[7,8] Our strategy for the development of a useful renin inhibitor is aimed at achieving high affinity and selectivity for the protease without incurring accompanying hydrolysis. Boger *et al.* designed potent renin inhibitors (pepstatin derivatives),[9] which contained an unusual amino acid, statine[10] [(3*S*,4*S*)-4-amino-3-hydroxy-6-methylheptanoic acid; see Fig. 1a]. Statine could possibly mimic a dipeptide,[11] wherein the amide bond (ψ[CONH]) is replaced by the ψ[CH(OH)CH_2] bond, as in pepstatin. Consequently, statine in the peptide chain blocks hydrolysis of several proteases, such as renin.

By the aid of comparative model-building techniques,[12] Akahane *et al.* attempted to design structures suitable for binding to renin.[13] Isopropyl (2*R*,3*S*)-4-cyclohexyl-2-hydroxy-3-{*N*-[(2*R*)-2-morpholinocarbonylmethyl-3-(1-naphthyl)-propionyl]-L-histidylamino}butyrate (KRI-1314) was developed as a potent human renin inhibitor (Fig. 1b)[14] and contained a novel cyclohexylnorstatine structure. This compound has the structure corresponding to the P4-P1′ site of angiotensinogen, and its two amide bonds are replaced by unusual bonds to suppress cleavage by proteases. KRI-1314 exhibits high inhibitory activity against renin (IC_{50} 2.4×10^{-9} mol dm^{-3}), though this compound shows no significant inhibitory activity against other proteases, such as cathepsin D and chymotrypsin.[15,16] Therefore, we thought it of interest to analyse the conformation of KRI-1314 in order to gain insight into the substrate specificity of renin. The conformational analysis would, furthermore, give useful information on inhibitor design based on the structure–activity relationship of the renin P4-P1′ site, owing to its mimic structure.

* Nomenclature of positions (P) is in accordance with a previous report (ref. 6).

Results and Discussion

Molecular Structure.—Fig. 2 shows the molecular conformation of KRI-1314, where backbone chain assumes an L-shape in the crystal. The morpholine (Mrp), an *N*-terminal residue, is linked by an amide bond with 2-(1-naphthylmethyl)succinate (Nps), and this linkage is a *retro-inverso*[17] type compared with that of normal peptides. The geometry of the amide bond is different from that of a normal peptide (Fig. 3a). However, the conformation of the Mrp^1 residue is similar to that of proline (*trans*-isomer), except for the steric hindrance from the side chain; the torsional angles related to the Mrp^1 residues are C(1′)–N(1A)–C(1)–C(2′) −175(1)° and N(1A)–C(1)–C(2′)–C(2A) 175.7(7)°. The main chain Nps^2–His^3 takes a *trans-zigzag* form. The torsional angles are C(1)–C(2′)–C(2A)–C(2) −65.1(6), C(2′)–C(2A)–C(2)–N(3) 144.4(7), C(2A)–C(2)–N(3)–C(3A) 168.8(7), C(2)–N(3)–C(3A)–C(3) −140.2(7), N(3)–C(3A)–C(3)–N(4) 167.9(7) and C(3A)–C(3)–N(4)–C(4A) 176.9(7)°. The backbone is twisted mainly at the cyclohexylnorstatine (Chs) and isopropyl ester (Isp) groups; C(3)–N(4)–C(4A)–C(4) −94.1(7) and N(4)–C(4A)–C(4)–C(5) 60.0(6)°. The

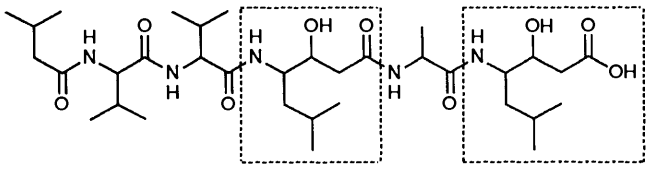

a

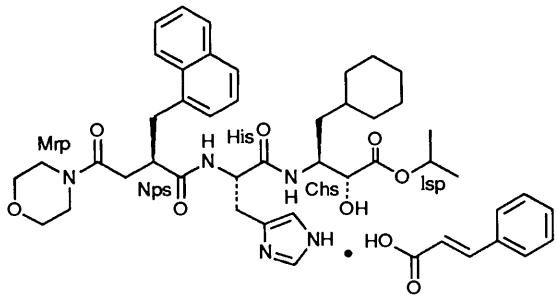

b

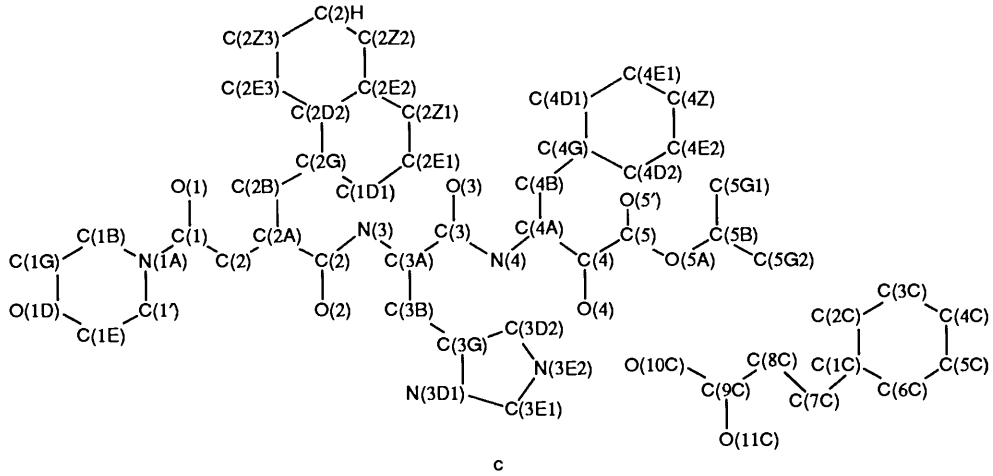

c

Fig. 1 Chemical structures of renin inhibitors and atomic numbering of KRI-1314. (a) Pepstatin (ref. 10), (b) KRI-1314, and (c) atomic numbering. Statine residues in (a) are boxed by dotted lines.

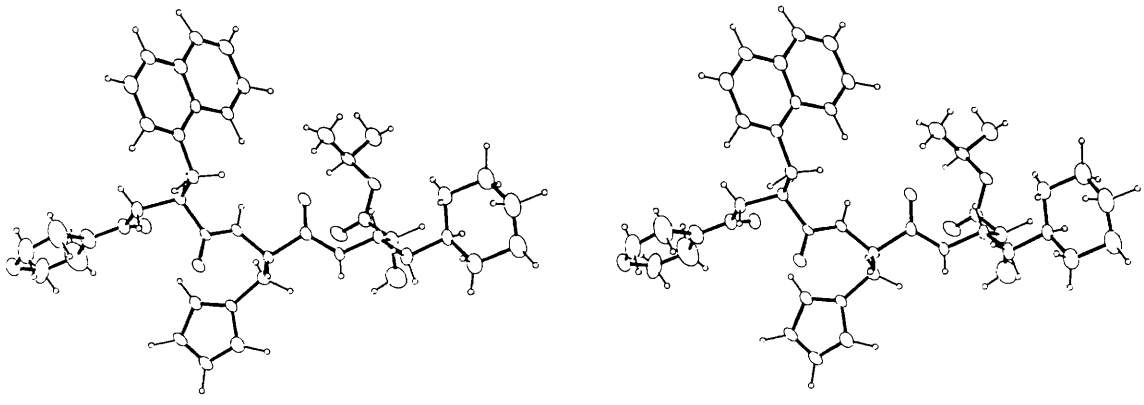

Fig. 2 Molecular conformation of KRI-1314

torsional angle C(4A)–C(4)–C(5)–O(5A) is 86.3(7)°, which corresponds to the peptide ω angle (normally 180°[18]). Although the conformation of KRI-1314 is different from that of the corresponding pepstatin derivative observed in the crystal structure,[19] it is interesting to note that a similarly twisted conformation of the backbone chain is observed at the statine residue of pepstatin bound to a carboxy proteinase.[20]

The torsional angles of side-chains are as follows; C(1')–N(1A)–C(1B)–C(1G) (χ_1) 10.0(1), C(2')–C(2A)–C(2B)–C(2G) (χ_2) −74.1(7), N(3)–C(3A)–C(3B)–C(3G) (χ_3) −69.6(6) and N(4)–C(4A)–C(4B)–C(4G) (χ_4) −168.8(7)°. The side-chains of Nps[2] and His[3] are orientated *gauche*. Although the Chs[4] side-chain is in a *trans* position, such a conformation avoids short contacts with the L-shaped main chain.

Geometry of Non-peptide Linkages.—Since the non-peptide linkages [C(1)–C(2') and C(4)–C(5)] of KRI-1314 are important for the inhibitory activity, the geometry observed was

compared with that of the normal peptide as shown in Fig. 3. The bond lengths and angles are slightly different. The bond lengths N(1A)–C(1) and C(1)–C(2′), however, correspond essentially to the respective C–N and C_α–N bond (Fig. 3a), and the spatial dispositions of the N(1A), C(1), O(1) and C(2′) atoms are almost the same as those of the corresponding atoms in the normal peptide. Although the partial double-bond character for the C(1)–C(2′) bond could not be expected to be similar to that of an amide bond (ψ[CONH]), the N(1A)–C(1)–C(2′)–C(2A) bond sequence achieves conformational planarity (torsional angle 176). Therefore, the linkage between Mrp[1] and Nps[2] is similar in size to that of an amide bond.

Contrary to this, however, the geometry of the linkage between the Chs[4] and Isp[5] moieties is significantly different from that of an amide bond (Fig. 3b). The hydroxy bond C(4)–O(4) is much longer than the C=O bond, and the C(4)–C(5) bond is also longer than the corresponding C–N bond. The existence of the oxygen atom O(5) causes a large spatial attraction from that of an amide bond. It could be that these structural characteristics help to achieve tight binding with renin, considering the strong inhibitory activity of KRI-1314.

In both linkages shown in Fig. 3 the geometries of the amide and ester bonds, which correspond to the scissile site of the protease substrate, disagree with those of the amide bond in the normal peptide. Furthermore, the O(4) atom of Chs[4] acts as both a donor and an acceptor for hydrogen bond formation, though this atom in the normal peptide acts only as an acceptor. The O(5) atom could be a hydrogen-bonding acceptor, while the nitrogen atom of the amide bond is a hydrogen-bonding donor. Thus, the arrangement of KRI-1314's polar atoms which are able to participate in hydrogen-bond formation is rather different from that of normal substrate polar atoms.

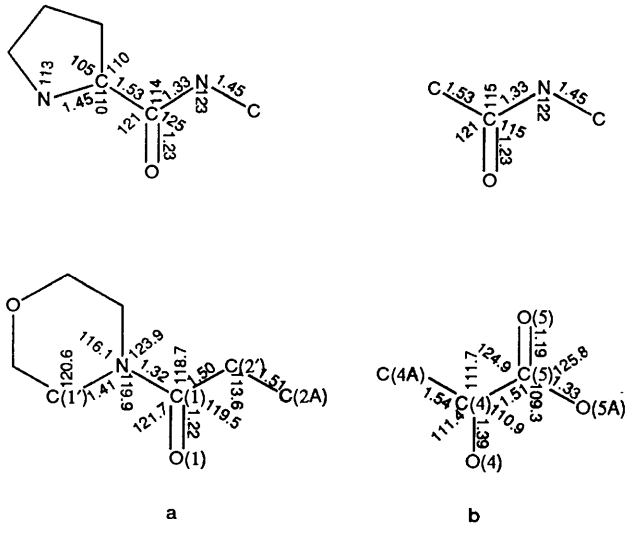

Fig. 3 Geometrical comparison of the non-peptide bond of KRI-1314 with a normal peptide bond, formed between the Mrp[1] and Nps[2] (a), and the Chs[4] and Isp[5] (b), residues. The geometry of the normal peptide corresponds to the upper pair, and that of the KRI-1314 to the lower pair, respectively.

Possible Conformation of P4–P1′ Site.—To compare the present conformation with that of the normal peptide corresponding to the P4–P1′ site, the model pentapeptide Pro-Phe-His-Leu-Val was built up by three-dimensional graphics and by energy minimization (see Experimental section). The superimposition of the pentapeptide with KRI-1314 is shown in Fig. 4. The white and black sticks represent the molecules of the model peptide and KRI-1314, respectively. Large deviations are observed in the residues of the non-peptide linkage. The Pro residue is rotated almost at right angles to the Mrp[1] residue. The side-chain of the Nps[2] residue takes a different conformation from that of the Phe side-chain, because of differences in ring bulkiness. The backbone chain is slightly shifted at the *C*-terminal residue. This would be due to the existence of the carboxy terminal in the model peptide. However, a good fit is achieved on the His[3] residue.

Molecular Association.—Intermolecular interactions are observed in the crystal. Fig. 5 shows the important molecular associations. Although no significant interaction is observed among the side-chains of the Mrp[1], Nps[2], Chs[4] and Isp[5] residues, electrostatic forces could exist between the His[3] residues of neighbouring molecules. The molecules in Fig. 5 are related to each other by the 2-fold screw axis, and projected on the imidazole rings of the His[3] residues. The imidazole rings overlap each other between the translated molecules, and the two ring planes are almost parallel; the dihedral angle between the rings is 18.3°. The interplanar spacing is 3.1–3.3 Å, which is somewhat shorter than the van der Waals separation distance (3.4 Å). Therefore, the imidazole rings could be stacked by partial π–π charge-transfer force. Furthermore, the carboxy oxygens of the cinnamic acids are hydrogen-bonded to the nitrogen atoms of the His[3] imidazole ring; N(3D1) · · · O(11C) 2.69(1) and N(3E2) · · · O(10C) 2.59(1) Å. Both the N(3D1) and N(3E2) atoms of the protonated imidazole ring act as donor atoms for the hydrogen bond, and the positive charge is delocalized on the ring. The histidine side-chain is thus linked with the cinnamic acid by two hydrogen bonds. A weak interaction is observed between the C(3E1) and keto oxygen O(2) atoms; C(3E1) · · · O(2) 3.08(1) Å. The water molecule of crystallization is located in the internal space between the KRI-1314 molecule and the cinnamic acid, and is hydrogen-bonded to both molecules; O(4) · · · W(1) 2.61(1), N(4) · · · W(1) 3.18(1), O(10C) · · · W(1) 2.64(1) and O(11C) · · · W(1) 2.55(1) Å. It is noticeable that the Chs[4] moiety of KRI-1314, which is linked with the water through a hydrogen bond, is the residue corresponding to the cleavage (P1) site[6] of angiotensinogen (discussed later).

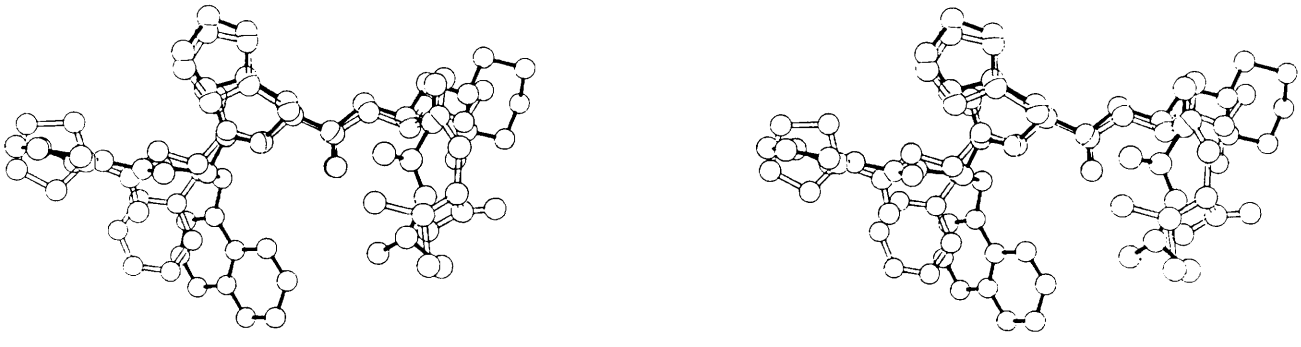

Fig. 4 Superimposition of KRI-1314 and model pentapeptide. The white and black sticks represent the model peptide and KRI-1314, respectively.

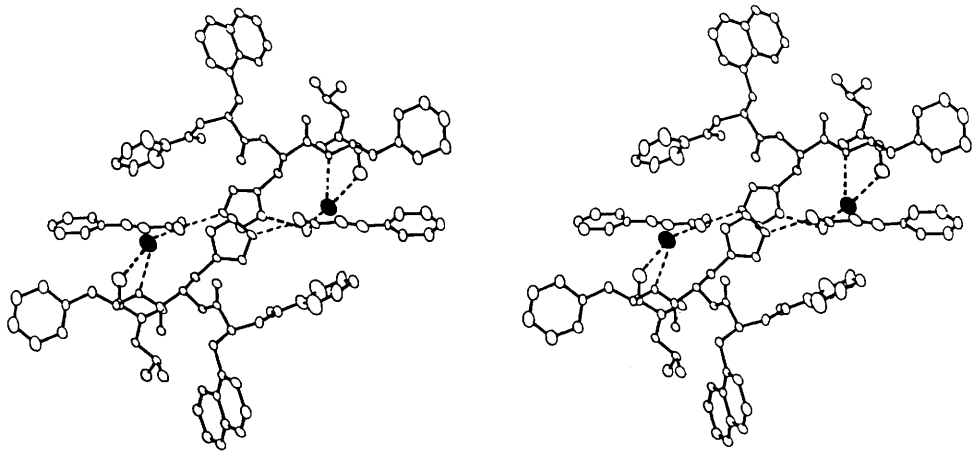

Fig. 5 Molecular association. Dotted lines represent hydrogen bonds. Filled circles represent water molecules of crystallization.

Possible Binding Mode to Renin.—The aforementioned intermolecular interactions (i, hydrophobicity of Nps and Chs side-chains; ii, stacking between His residues; iii, hydrogen bonds with cinnamic acid; and iv, hydrogen bonds with water) are important in considering the possible binding of the inhibitor to renin, as follows: (1) The three-dimensional structure of recombinant renin has been reported,[21] where the active site region consists of the hydrophobic residues of leucine, isoleucine and valine. These amino acid residues could generate hydrophobic forces for the interaction with the KRI-1314 molecule. The residues Nps[2] and Chs[4] have more bulky and hydrophobic side-chains compared with the normal amino acids. These side-chains would be convenient for binding to renin *via* hydrophobic interaction. (2) Potent peptide inhibitors of renin usually contain a histidine residue at the position corresponding to the P2 site.[7,8] The present simulation suggested that the conformation of the His[3] residue was similar to that in the renin inhibitor KRI-1314 and that in the model substrate. Since it has already been shown that there were electron-rich amino acids such as tryptophan and tyrosine in the active-site region of renin,[21] they could be expected to bind the histidine side-chain by a stacking interaction, just like the interaction observed in the present crystal structure. (3) In the present crystal structure, the hydrogen bonds were formed between the His[3] residue and the carboxy group of the cinnamic acid. Judging from molecular models of human renin,[12,13] it is most probable that the His[3] residue of KRI-1314 is fixed by a hydrogen bond with the serine-233 OH side-chain of renin. In addition to the stacking interaction of the His[3] imidazole rings (ii, above), such a hydrogen bond would enhance the specificity of the inhibitor to renin.[22] (4) For the hydrolysis by aspartic protease a tetrahedral complex model has been proposed, where the substrate interacts with the Asp and Gly residues, and with a water molecule which locates at a position near to the amide bond of the cleavage site (P1).[20] The water molecule of crystallization is likely to be that one used for the hydrolysis of the substrate. In the present crystal structure, the water of crystallization is located 2.6 Å away from the O(4) atom of the Chs[4] residue corresponding to the P1 site, and participated in the formation of hydrogen bonds. Furthermore, (5) the dispositions of hydrogen bond-donor and -acceptor atoms on the Mrp[1] and Chs[4] residues could give a potential for diversity of binding of the inhibitor to the active site of renin, compared with the substrate.

Experimental

Crystal Data.—$C_{38}H_{51}N_5O_7 \cdot C_9H_8O_2 \cdot H_2O$, molecular weight in an asymmetric unit 856.04, monoclinic, $P2_1$, a = 23.076(8), b = 6.200(1), c 16.582(7) Å, β = 108.64(5)°, V = 2248(1) Å^3, Z = 2, D_x = 1.255 g cm^{-3}.

Data Collection.—Attempted crystallization of KRI-1314 from several solvents and with several different counter-anion salts finally yielded needle crystals of KRI-1314 from aq. methanol solution as a cinnamic acid salt monohydrate by slow evaporation at room temperature. The dimensions were *ca.* 0.07 × 0.07 × 0.6 mm along edges. Cell constants were determined by a least-squares fitting of 24 reflections on a Rigaku diffractometer equipped with a graphite monochromator using Cu-Kα radiation (λ 1.5418 Å). Intensities were collected by the ω–2θ scan mode using variable speed (2–4° min^{-1}). Standard reflections monitored during the measurement indicated stable X-ray output and no significant decay of the crystal. The data were corrected for Lorentz and polarization effects. Absorption correction was also applied according to the method[23] based on a φ-scan along the b-axis of the crystal. Unique data of 3234 reflections were measured within 2θ 110°. The reflective intensities of this crystal largely decreased depending on the 2θ angle, and reflections for $2\theta > 110°$ were weak because of the small size of the crystal.

Structure Determination and Refinement.—The backbone structure was solved by MULTAN87,[24] and the remaining atoms were picked out from successive weighted Fourier maps. The structure was refined by the 'blocked' full-matrix least-squares method using SHELX-76[25] minimizing the quantity $\Sigma w(|F_o| - |F_c|)^2$. Anisotropic temperature factors were applied for non-hydrogen atoms. Hydrogens were calculated at geometrically ideal position, and were included in the refinement with isotropic temperature factors. The y-co-ordinate of the N(1) atom was fixed during the refinement to avoid divergence of the molecular co-ordinates along the b-axis. In the final cycle, the weight was calculated as $w = 1.0/[\sigma^2(F_o) + 0.000\,63F_o^2]$, and R and R_w were reduced to 0.0692 and 0.0658 for 2475 reflections with $F_o > 3.0\sigma(F_o)$, where $\sigma(F_o)$ was the standard deviation in F_o. All crystallographic calculations were performed on a MicroVAX-II computer at Osaka University of Pharmaceutical Sciences. The obtained atomic co-ordinates are listed in Table 1,* and the atomic numbering used in this work is indicated in Fig. 1c. The averaged standard deviations for bond lengths and angles are 0.1 Å and 0.6°, respectively. Owing to the

* *Supplementary data* (see section 5.6.3 of Instruction for Authors, in the January issue). Anisotropic temperature factors of non-hydrogen atoms, the hydrogen atomic co-ordinates, bond lengths and angles, torsion angles, and hydrogen bonds and short contacts have been deposited at the Cambridge Crystallographic Data Centre.

Table 1 Fractional co-ordinates with esds in parentheses

Atom	x	y	z	Atom	x	y	z
C(1')	0.0395(6)	0.591(2)	0.178(3)	C(3)	0.2561(3)	0.519(1)	0.6746(4)
N(1A)	0.0797(3)	0.7599[a]	0.2159(5)	O(3)	0.3028(2)	0.499(1)	0.6557(3)
C(1B)	0.0687(6)	0.967(2)	0.1707(8)	N(4)	0.2541(2)	0.493(1)	0.7537(3)
C(1G)	0.0212(6)	0.988(2)	0.1101(7)	C(4A)	0.3070(3)	0.434(1)	0.8264(4)
O(1D)	−0.0179(3)	0.820(1)	0.0676(3)	C(4B)	0.3044(3)	0.556(2)	0.9026(4)
C(1E)	−0.0069(6)	0.625(2)	0.1099(7)	C(4G)	0.3617(3)	0.550(2)	0.9816(4)
C(1)	0.1251(4)	0.725(2)	0.2867(5)	C(4D1)	0.3474(4)	0.663(2)	1.0546(6)
O(1)	0.1377(2)	0.544(1)	0.3158(3)	C(4E1)	0.4031(6)	0.658(3)	1.1380(7)
C(2')	0.1640(3)	0.912(1)	0.3294(4)	C(4Z)	0.4549(6)	0.775(2)	1.1154(7)
C(2A)	0.2115(3)	0.854(1)	0.4132(4)	C(4E2)	0.4708(5)	0.652(2)	1.0439(7)
C(2B)	0.2551(3)	1.042(1)	0.4495(4)	C(4D2)	0.4176(4)	0.639(2)	0.9644(5)
C(2G)	0.3007(3)	1.080(1)	0.4033(4)	C(4)	0.3098(3)	0.189(1)	0.8402(5)
C(2D1)	0.2933(3)	1.252(1)	0.3490(5)	O(4)	0.2599(3)	0.115(1)	0.8623(4)
C(2E1)	0.3354(4)	1.292(2)	0.3019(5)	C(5)	0.3150(4)	0.070(1)	0.7635(5)
C(2Z1)	0.3833(3)	1.152(2)	0.3124(5)	O(5')	0.2727(2)	0.003(1)	0.7066(4)
C(2E2)	0.3934(3)	0.980(2)	0.3685(5)	O(5A)	0.3736(2)	0.056(1)	0.7686(3)
C(2Z2)	0.4433(3)	0.837(2)	0.3785(5)	C(5B)	0.3881(3)	−0.039(1)	0.6924(5)
C(2H)	0.4523(3)	0.676(2)	0.4320(6)	C(5G1)	0.4056(3)	0.141(2)	0.6464(6)
C(2Z3)	0.4124(4)	0.630(2)	0.4822(5)	C(5G2)	0.4387(4)	−0.198(2)	0.7290(5)
C(2E3)	0.3631(3)	0.764(2)	0.4711(5)	W(1)[b]	0.1464(3)	0.211(2)	0.7798(6)
C(2D2)	0.3503(3)	0.942(1)	0.4146(4)	C(1C)	0.1734(3)	0.733(2)	0.9981(4)
C(2)	0.1811(3)	0.787(1)	0.4776(4)	C(2C)	0.2058(4)	0.920(2)	1.0310(5)
O(2)	0.1364(2)	0.8879(9)	0.4848(3)	C(3C)	0.2374(4)	0.949(2)	1.1169(5)
N(3)	0.2087(2)	0.633(1)	0.5307(3)	C(4C)	0.2341(4)	0.775(2)	1.1685(6)
C(3A)	0.1954(3)	0.564(1)	0.6065(4)	C(5C)	0.2027(4)	0.585(2)	1.1385(5)
C(3B)	0.1573(3)	0.358(1)	0.5899(4)	C(6C)	0.1709(3)	0.564(2)	1.0521(5)
C(3G)	0.0928(3)	0.383(1)	0.5320(4)	C(7C)	0.1419(4)	0.663(3)	0.9155(5)
N(3D1)	0.0454(3)	0.421(1)	0.5657(4)	C(8C)	0.1263(4)	0.726(2)	0.8453(5)
C(3E1)	−0.0066(3)	0.425(1)	0.5026(6)	C(9C)	0.0919(5)	0.706(2)	0.7591(5)
N(3E2)	0.0049(2)	0.399(1)	0.4310(4)	O(10C)	0.0829(3)	0.865(2)	0.7122(5)
C(3D2)	0.0671(3)	0.371(1)	0.4478(4)	O(11C)	0.0730(4)	0.527(2)	0.7307(4)

[a] Fixed. [b] W Represents the water molecule of crystallization.

relatively low number of reflections compared with the atom number of the molecule, these values are rather high, and their bonding parameters are somewhat imprecise. However, this would not seriously affect the molecular conformation discussed in the text.

Molecular Modelling and Fitting of P4-P1′ *Peptide.*—The pentapeptide Pro-Phe-His-Leu-Val (the P4-P1′ site of angiotensinogen[6]) was built up by three-dimensional graphics on an IRIS computer. The peptide structure was energy-refined by the molecular mechanics force-field method[26] on the CHEMLAB system.[27] The molecular steric energy converted to −24.8 kcal mol^{-1}.*

The molecular superposition between the pentapeptide and KRI-1314 was fitted by a least-squares method. For the fitting calculations, the root-mean-square error was within 0.88 Å between the main-chain atoms of both molecules.

* 1 cal = 4.184 J.

References

1 M. J. Peach, *Physiol. Rev.*, 1977, **57**, 313.
2 R. R. Smeby, *Chemistry and Biochemistry of Amino Acids, Peptides, and Proteins*, ed. B. Weinstein, Marcel Dekker, New York, 1978, vol. 5, p. 117.
3 L. C. Skeggs, F. E. Dorer, M. Levine, K. E. Lentz and J. R. Kahm, *The Renin Angiotensin System*, ed. J. A. Johnson and R. R. Anderson, Plenum, New York, 1980, p. 1.
4 M. A. Ondetti, B. Rubin and B. W. Cushman, *Science*, 1976, **196**, 441.
5 A. A. Patchett, E. Harris, E. W. Tristam, M. J. Wycratt, M. T. Wu, D. Taub, E. R. Peterson, T. J. Ikeler, J. TenBroke, L. G. Payne, D. L. Ondeyka, E. D. Thorset, W. J. Greenlee, S. R. Lohr, R. D. Hoffsommer, H. Joshua, W. W. Ruyle, J. W. Rothrock, S. D. Aster, A. L. Maycock, F. M. Robinson, R. Hirschmann, C. S. Sweet, E. H. Ulm, D. H. Gross, T. C. Vassil and C. A. Stone, *Nature (London)*, 1980, **228**, 280.
6 I. Schechter and A. Berger, *Biochem. Biophys. Res. Commun.*, 1968, **32**, 898.
7 R. Guegan, J. Diaz, C. Cazaubon, M. Beaumont, C. Carlet, J. Cément, H. Demarne, M. Mellet, J.-P. Richaud, D. Segondy, M. Vedel, J.-P. Gagnol, R. Roncucci, B. Castro, P. Corvol, G. Evin and B. P. Roques, *J. Med. Chem.*, 1986, **29**, 1152.
8 M. G. Bock, R. M. DiPardo, B. E. Evans, K. E. Rittle, J. S. Boger, R. M. Freidinger and D. F. Veber, *J. Chem. Soc., Chem. Commun.*, 1985, 109.
9 J. Boger, N. S. Lohr, E. H. Ulm, M. Poe, E. H. Blaine, G. M. Fanelli, T.-Y. Lin, L. S. Payne, T. W. Schorn, B. I. LaMont, T. C. Vassil, I. I. Stabilito, D. F. Veber, D. H. Rich and A. S. Bopari, *Nature (London)*, 1983, **303**, 81.
10 W. Umezawa, T. Aoyagi, H. Morishima, M. Matsuzaki, M. Hamada and T. Takeuchi, *J. Antibiot.*, 1970, **23**, 259.
11 J. Boger, *Peptides Structure and Function*, Proceedings of the 8th American Peptide Symposium, ed. V. J. Hruby and D. H. Rich, Pierce Chemical Co., Rockford, IL, 1983, p. 569.
12 K. Akahane, H. Umeyama, S. Nakagawa, I. Moriguchi, S. Hirose, K. Iizuka and K. Murakami, *Hypertension*, 1985, **7**, 3.
13 K. Akahane, T. Kamijo, K. Iizuka, T. Taguchi, Y. Kobayashi, Y. Kiso and H. Umeyama, *Chem. Pharm. Bull.*, 1988, **36**, 3447.
14 K. Iizuka, T. Kamijo, H. Harada, K. Akahane, T. Kubota, H. Umeyama and Y. Kiso, *J. Chem. Soc., Chem. Commun.*, 1989, 1678; H. Harada, A. Iyobe, A. Tsubaki, T. Yamabuchi, K. Hirata, T. Kamijo, K. Iizuka and Y. Kiso, *J. Chem. Soc., Perkin Trans. 1*, 1990, 2497.
15 K. Iizuka, T. Kamijo, H. Harada, K. Akahane, T. Kubota, Y. Etoh, I. Shimaoka, A. Tsubaki, M. Murakami, T. Yamaguchi, A. Iyobe, H. Umeyama and Y. Kiso, *Chem. Pharm. Bull.*, 1990, **38**, 2487.
16 K. Iizuka, T. Kamijo, H. Harada, K. Akahane, T. Kubota, H. Umeyama, T. Ishida and Y. Kiso, *J. Med. Chem.*, 1990, in the press.
17 H. Harada, K. Iizuka, T. Kamijo, K. Akahane, R. Yamamoto, Y. Nakano, A. Tsubaki, T. Kubota, I. Shimaoka, H. Umeyama and Y. Kiso, *Chem. Pharm. Bull.*, 1990, in the press.
18 G. E. Schulz and R. H. Schirmer, *Springe Advanced Texts in Chemistry: Principles of Protein Structure*, ed. C. R. Cantor, Springer-Verlag, New York, 1979, p. 1.

19 G. Precigoux, S. Geoffre and E. Quvrad, *Acta Crystallogr., Sect. C*, 1986, **42**, 721.
20 R. Bott, E. Subramanian and R. D. Davies, *Biochemistry*, 1982, **21**, 6956.
21 A. R. Sielecki, K. Hayakawa, M. Fujinaga, E. P. M. Murphy, M. Fraster, A. K. Muir, C. T. Carilli, J. A. Lewicki, J. D. Baxter and M. N. G. James, *Science*, 1989, **243**, 1346.
22 K. Iizuka, T. Kamijo, T. Kubota, K. Akahane, H. Umeyama and Y. Kiso, *J. Med. Chem.*, 1988, **31**, 701.
23 A. C. T. North, P. C. Phillips and F. S. Mathews, *Acta Crystallogr., Sect. A*, 1968, **24**, 351.
24 T. Debaerdemaeker, G. Germain, P. Main, C. Tate and M. M. Woolfson, MULTAN87, Computer Programs for the Automatic Solution of Crystal Structures from X-Ray Diffraction Data, Universities of York, England, and Louvain, Belgium, 1987.
25 G. M. Sheldrick, SHELX-76, Program for Crystal Structure Determination, University of Göttingen, Göttingen, 1976.
26 A. J. Hopfinger and R. A. Pearlstein, *J. Comput. Chem.*, 1984, **5**, 486.
27 CHEMLAB-II, A Molecular Modeling Software System, Molecular Design, Ltd., San Diego, CA, 1986.

Paper 0/04527F
Received 8*th October* 1990
Accepted 22*nd November* 1990